Intraductal patient-derived xenografts of estrogen receptor α-positive (ER+) breast cancer recapitulate the histopathological spectrum and metastatic potential of human lesions

Maryse Fiche, Valentina Scabia, Patrick Aouad, Laura Battista, Assia Treboux, Athina Stravodimou, Khalil Zaman, Valérian Dormoy, Ayyakkannu Ayyanan, George Sflomos, et al.

Intraductal patient derived xenografts of estrogen receptor α positive (ER+) breast cancer recapitulate the histopathological spectrum and metastatic potential of human lesions

Maryse Fiche[1,*], Valentina Scabia[2,*], Patrick Aouad[2], Laura Battista[2], Assia Treboux[3], Athina Stravodimou[3], Khalil Zaman[3], RLS[4], Valerian Dormoy[5], Ayyakkannu Ayyanan[2], George Sflomos[2], and Cathrin Brisken[2, 6]

[1]International Cancer Prevention Institute, CH-1066 Epalinges, Switzerland

[2]Swiss Institute for Experimental Cancer Research, School of Life Sciences, Ecole Polytechnique Fédérale de Lausanne, CH-1015 Lausanne, Switzerland

[3]Centre Hospitalier Universitaire Vaudois, University Hospital of Lausanne, CH-1011 Lausanne, Switzerland

[4]Réseau Lausannois du Sein, Rue de la Vigie 5, CH-1004 Lausanne, www.rlds.ch

[5] Present address: INSERM UMR_S1250, Université de Reims Champagne-Ardenne (URCA), 51092 Reims, France

[6] Correspondence to: Cathrin Brisken, Swiss Institute for Experimental Cancer Research, School of Life Sciences, Ecole Polytechnique Fédérale de Lausanne, CH-1015 Lausanne, Switzerland. Email: cathrin.brisken@epfl.ch

* these authors contributed equally

Short title: Intraductal patient dervived xenografts of hormone-sensitive breast cancers

Conflict of interest statement: The authors declare no conflict of interest.

This article has been accepted for publication and undergone full peer review but has not been through the copyediting, typesetting, pagination and proofreading process, which may lead to differences between this version and the Version of Record. Please cite this article as doi: 10.1002/path.5200

Abstract

Estrogen receptor α positive (ER^+) or "luminal" breast cancers (BC) were notoriously difficult to establish as patient-derived xenografts (PDXs). We and others recently demonstrated that the microenvironment is critical for ER^+ tumor cells; when grafted as single cells into milk ducts of NOD Scid gamma (NSG) females >90% of ER^+ tumors can be established as xenografts and recapitulate many features of the human disease *in vivo*. This intra-ductal (ID) approach holds promise for personalized medicine, yet human and murine stroma are organized differently and this and other species specificities may limit the value of this model. Here, we analyzed 21 ER^+ ID-PDXs histopathologically. We find that ID-PDXs vary in extent and define four histopathological patterns: flat, lobular, *in situ*, and invasive, which occur in pure and combined forms. The ID-PDXs replicate earlier stages of tumor development than their clinical counterparts. Micrometastases are already detected when lesions appear *in situ*. Tumor extent, histopathological patterns and micrometastatic load correlate with biological properties of their tumors of origin. Our findings add evidence to the validity of the intraductal model for *in vivo* studies of ER^+ breast cancer and raise the intriguing possibility that tumor cell dissemination may occur earlier than currently thought.

Keywords: intraductal xenografts, luminal breast cancer, preclinical model, patient-derived xenografts, ductal carcinoma *in situ*, micrometastasis

Introduction

Breast cancer (BC) is a frequent disease worldwide [1]. Over 75% of BCs express ER in >1% of the tumor cells by immunohistochemistry (IHC) [2] and overlap with luminal A and B subtypes defined by global gene expression [3,4] exhibiting low *versus* high proliferative indices and distant recurrence rates [5]. Twenty percent of patients experience distant recurrence and cancer-related death [6]. Overtreatment of early disease and endocrine resistance are additional problems concerning this subgroup [7]. A lack of preclinical models hampered progress in understanding the biology of luminal tumors and development of new therapies. Genetically engineered mouse models mostly develop ER^- tumors, and few ER^+ BC cell lines grow *in vivo* requiring nonphysiological estrogen supplements [8]. PDXs are increasingly used but difficult to establish from ER^+ tumors [8]. We and others showed that the microenvironment is a major determinant of luminal BC cells and that take rates increase dramatically when luminal BC cells are grafted to mouse milk ducts [9]. They grow without estrogen supplementation recapitulating many features of their clinical counterpart [9,10]. Yet, mammary stroma and endocrine milieu differ beween women and mice. To assess the impact of the mouse host on the biology of the engrafted human cells, we analyzed 21 ID-PDXs histopathologically.

Materials and Methods

The study was approved by the Commission cantonale d'éthique de la recherche sur l'être humain (CER-VD 38/15), patients signed informed consent. Animal experiments were performed in accordance with protocol 1861.3 approved by Service de la Consommation et des Affaires Vétérinaires, Canton de Vaud, Switzerland. After inking of margins and macroscopic assessment, part of tumor tissue was taken by the pathologist (MF), transported to the laboratory in DMEM/F12, mechanically and enzymatically dissociated to single cells, lentivirally transduced with luciferase-GFP and injected into teats of 10-week-old NSG females [9]. *In vivo* growth was monitored biweekly by bioluminescence. Engrafted glands were dissected, fixed in buffered formalin for 2 h and paraffin-embedded. Four μm sections were cut and number 1, 7, and 15 stained with Hemalum/Eosin (H&E). ALU staining unequivocally identified human cells when required. IHC was performed on Discovery

Ventana ULTRA [9]. Micrometastatic load was calculated as percentage of bioluminescence+ organs of all organs collected.

Results

Tumor cells from 21 patients were intra-ductal grafted to 88 mice in 220 glands after lentiviral transduction with luciferase-GFP (Figure 1A, B, Table S1). Mice were sacrificed when radiance >10E8 so tumor cells are readily detectable. Micrometastases, consisting of < 30 cells (Figure 1C), were detected in 90% of the 31 mice analyzed by *ex vivo* radiance measurements on various organs revealing bones as the most frequent site of tumor cell seeding, followed by lungs, brain and liver (Figure 1D). Tumor extent assessed semi-quantitatively on H&E stained sections varied with ≥70% of ducts distended by human cells in 6/21 PDXs (Figure S1A), tumor cell foci occupying 20-60% or < 5% of the ductal tree in 10 and 5 PDXs, respectively (Figure S1B, C).

While the distribution of ER^+ and PgR^+ indices in primary tumors (PTs) and PDXs were similar (Table S1, Figure S2A, B) they differed by >10% in 5 and 12 pairs, respectively, consistent with higher inter- and intratumor variability of PgR staining in clinical samples (Figure S2C, D). HER2 status was IHC 3+ in 2/3 PDXs corresponding to IHC 3+ PTs including one confirmed by FISH. A PT with a IHC 2+ score and focal gene amplification was negative in the PDX, suggesting clonal outgrowth [12].

The PDXs showed 4 distinct architectural patterns reminiscent of human breast disease: flat (F), lobular (LOB), *in situ* (IS), and invasive (INV) in pure form or mixed. The **F** pattern (Figure 2A-E), resembled columnar cell changes and flat epithelial atypia, an early premalignant alteration [11,12], showing a monolayer lining of variably dilated mouse ducts (Figure 2A) with large columnar cells, mild nuclear pleomorphism and abundant eosinophilic cytoplasm forming apical "snouts" (Figure 2B). It associated with foci of intraductal proliferation of low nuclear grade tumor cells in a cribriform pattern similar to atypical ductal hyperplasia (Figure 2E) [11]. Strong and diffuse ER (Figure 2D) and PgR expression (Figure 2E) were observed and interpreted as early "colonization" of murine ducts by human tumor cells.

The LOB pattern was characterized by tumor cell growth within the ductal walls, like pagetoid spread of lobular carcinoma *in situ* (LCIS) (Figure 2F, G, Figure S3) [11,13], associated with intracellular clear, mucin-like vacuoles bestowing a signet-ring cell-like appearance on the tumor cells (Figure 2F). Interestingly, 4/5 lobular PDXs corresponded to this pattern, no typical LCIS was observed, instead four of them exhibited the F pattern and four exhibited the LOB pattern. In the human breast also, columnar cell changes and lobular neoplasia are frequent in "low grade" precursor lesions of both ductal and lobular subtypes [14,15]. The only case of pleomorphic lobular carcinoma showed LOB and F patterns with a 20% proliferative fraction (Fig. 1B).

The IS pattern showed varying degrees of filling of the ductal lumen by tumor cells (Figure 2H-O) and resembled ductal carcinoma *in situ* (DCIS). It encompassed combinations of different degrees of nuclear pleomorphism and architectural patterns, like cribriform (Figure 2H-J) or solid with or without *comedo*necrosis (Figure 2K-O) [11]. An ER^+ $HER2^+$ PDX showed large tumor extent, high nuclear pleomorphism, *comedo* architecture, high proliferation rate (Figure 2M) and HER2 overexpression (Figure 2O).

Although the tumor cells were derived from invasive PTs, only 1/3 of the PDXs had an INV pattern with tumor cells detected outside the host ducts, either isolated or in small clusters (Figure 2P-R). Thus, intraductal xenografts replicate earlier stages than the original PT, nevertheless, micrometastases were present in 90% of the mice and in all the 16 analyzed PDXs (Table S1).

Next, we assessed how the biological features of the PDXs related to the prognostic characteristics of their clinical counterparts. According to a 20% Ki67 IHC cut-off based on clinical practice [16], the PT series comprised 7 luminal A-like (Ki67 <20%) and 14 luminal B-like (Ki67 $\geq$20%) cases; 4 of the latter were HER2+. In luminal A-like cases, the F pattern was observed in 6/7 PDXs, pure in 3 cases, mixed with IS in 1 and with LOB pattern in 2 cases. No INV pattern was found and the IS pattern only in one case (Table 1, Figure 3A). The F pattern was observed in 9/14 luminal B-like cases, all NST, with only 2 pure (Figure 3A). The INV pattern was detected in 6/14, IS and INV patterns were combined in 4/14. Thus, the F pattern tended to be present in luminal A-like BC derived PDXs. IS and INV patterns on the contrary were observed, with or without associated F pattern, in PDXs

obtained from the more aggressive luminal B-like subtype. Micrometastatic burden was higher in mice engrafted with luminal B-like than luminal A-like PTs (Figure 3B).

Tumor extent did not correlate with the time the grafted cells spent in the hosts (Figure 3C) nor with the number of cells injected (Figure 3D) but with *in vivo* growth rates (Figure 3E) and Ki67 index in PT (Figure 3F). The proliferative indices in PTs also correlated with *in vivo* growth rates (Figure 3G) and micrometastatic load (Figure 3H). Thus, tumor extent relates to PT biology rather than to engraftment modalities; growth rates and micrometastatic burden reflect Ki67 index and hence patient prognosis.

Discussion

The intraductal-PDXs of ER^+ BCs in this study reproduce the spectrum of ER^+ DCIS with different architectures: solid, comedo and cribriform, combined with various degrees of nuclear pleomorphism, necrosis and calcification [11,13,17]. Several precursor lesions, like flat epithelial atypia, atypical ductal hyperplasia, pagetoid growth of LCIS were observed, while typical aspects of LCIS were not. Invasive cancer occurred only as small foci and no true invasive lobular carcinomas or other special subtypes were observed in the 21 PDXs under study.

Hence, most histopathologic features are tumor cell-intrinsic and not determined by stroma or systemic factors, which differ between humans and mice. The observation that two-thirds of the PDXs derived from invasive cancers represent earlier lesions suggests that engrafted cells re-start growth intraductally, recapitulating different steps with a prolonged stage of non-invasive growth as they likely did in the patient‘s breast years before diagnosis. This is important to consider when using the model in personalized medicine [9].

While the typical F, LOB and IS patterns are readily identified, some morphological aspects of ER^+ intraductal-PDX are more difficult to classify. This concerns dispersed foci of human cells lining the wall of small mouse ducts, with neither apical snouts nor cystic duct dilation. We classified these as F but speculate that they will evolve into a different pattern. While most (15/21) PDXs have some F pattern, it tends to be pure in luminal A-derived PDXs whereas IS and INV patterns are detected when luminal B cells were engrafted. Furthermore, proliferative indices of PTs are maintained in the PDXs.

Thus, the heterogeneity of luminal tumors is preserved. This is especially important regarding the clinical problem of overtreatment; the model may help identify tumors with low aggressiveness and/or a high level of responsiveness to endocrine therapy.

Figure legends

Figure 1. Intraductal ER^+ breast cancer patient-derived xenografts. (A) Experimental scheme of PDX establishment and follow-up. PTs are dissociated to single cells, which are subsequently transduced with lentivirus encoding GFP and luciferase. The infected cells are injected intraductally in multiple glands and their *in vivo* growth is monitored by bioluminescence. The mice are euthanized and the presence of metastases is assessed by bioluminescence in brain, lungs, bones, liver. Analysis of spleen, intestine and other internal organs was negative. (B) Table reporting PT and PDX characteristics. (C) H&E stained section of a micrometastasis*** in the lung, consisting of atypical cells with large nuclei. Inset: IHC staining for ER (brown) with Mayer's haematoxylin counterstain of an adjacent section revealing the ER^+ tumor cells in the ER^- lung tissue. Scale bars 35 μm. (D) Numbers of different organs (n=88) in 31 xenografted mice bearing micrometastases.

Fiche et al. Figure 1

A

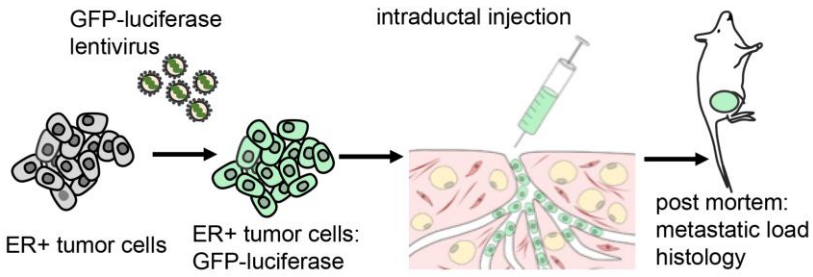

B

Primary tumor				Patient-derived xenograft (PDX)				
Case	Histol. type	Ki67%	HER2	Tumor extent (%)	Pattern **F**	Pattern **IS**	Pattern **INV**	Pattern **LOB**
61	NST	90	-	100		+	+	
63	NST	25	-	80	+		+	
65	NST	17	-	60	+			
67	NST	29	-	85		+		
68	NST	20	-	3		+ f	+	
69	Lobular	16	-	40	+			+
73	Lobular	25	+	30	+			+
76	NST	80	-	80	+		+	
78	Lobular	10	-	70				+
79	NST	40	+	10	+	+		
81	NST	30	-	2	+			
84	Mixed	10	-	2	+	+		
85	Lobular	<5	-	4	+			
86	Lobular	<5	-	50	+			+
87	NST	90	-	50	+	+f		
91	NST	25	-	50	+	+		
92	NST	20	+	60	+			
93	NST	20	-	30	+	+		
95	NST	90	+	100		+	+	
96	NST	10	-	3	+			
99	NST	50	-	50		+	+	

C

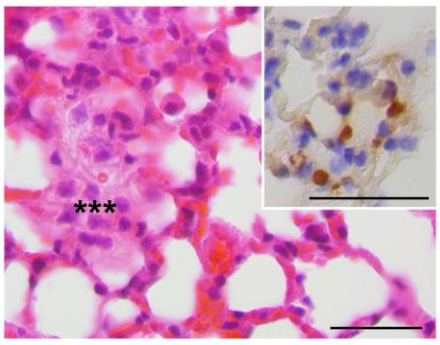

D

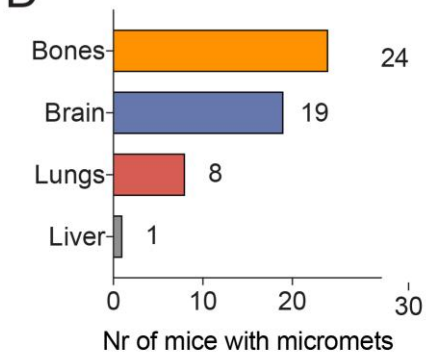

Figure 2. ID-PDXs exhibit four morphological patterns by H&E and IHC. (A-E) Flat (F) pattern. (A-C) Human tumor cells cover the wall of variably dilated ducts forming a monolayer of large cylindrical cells with small nuclei, eosinophilic cytoplasm and apical cytoplasmic "snouts" reminiscent of columnar cell changes and flat epithelial atypia in the human breast. (D, E) Estrogen

(ER) (D) and PgR (E) are strongly and diffusely expressed by human cells. (E) Focally, transition between the F pattern and cellular bridges similar to human atypical ductal hyperplasia is seen. (F-G) Lobular (LOB) pattern. (F) The mouse ductal epithelium is replaced by human cells harboring two associated phenotypes: i) large cells with a "signet ring cell" appearance (a large cytoplasmic vacuole displaces an enlarged nucleus toward the periphery of the cell) grow within the ductal wall in a "pagetoid" manner; ii) smaller cohesive cubo-cylindrical cells lining the ductal lumen. (G) ER is expressed in most large cells and in a few cylindrical cells. (H-O) In Situ (IS) pattern. Human tumor cells fill the ductal lumen. (H-J) Some IS PDXs exhibit a cribriform architectural pattern, mild nuclear pleomorphism, low proliferation index (Ki67) (I), and diffuse strong ER (J). (K-O) One PDX exhibits a solid growth with comedonecrosis (K), marked nuclear pleomorphism (L, N), high proliferation index (Ki67) (M), and HER2 overexpression (O). (P-R) Invasive pattern (INV). Tumor cells diffusely expressing ER fill the dilated mouse ductal tree (P, Q), and grow outside the ducts in small clusters surrounded by collagen (P, R arrows). Scale bars 100 μm.

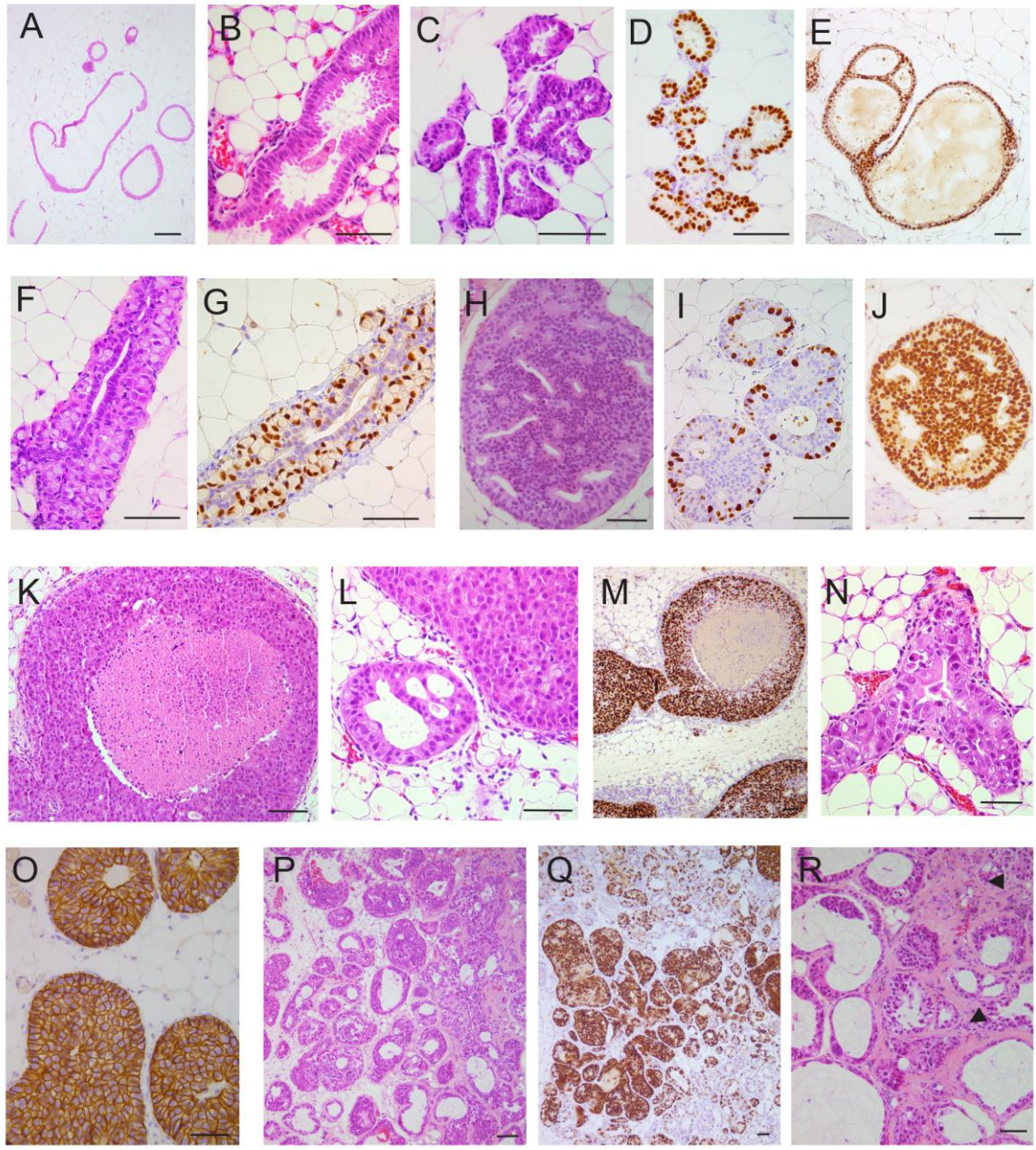

Figure 3. Characterization of *in vivo* growth. (A) Distribution of histological patterns within each subtype. (B) Micrometastatic burden expressed as percentage of positive organs in each recipient in luminal A (LumA) versus luminal B (LumB) derived PDXs. (C-F) Pearson correlation of tumor extent against (C) time of PDX growth *in vivo*, expressed in days after injection, (D) initial number of cells injected per gland, (E) *in vivo* cell growth expressed as fold change radiance relative to the first day of measurement (log10) and (F) Ki67 index of the primary tumor. (G,H) Pearson correlation of primary tumor Ki67% with (G) *in vivo* monitored growth and with (H) micrometastatic burden the percentage of organs affected by metastases within each case as determined by bioluminescence.

Fiche et al.

Figure 3

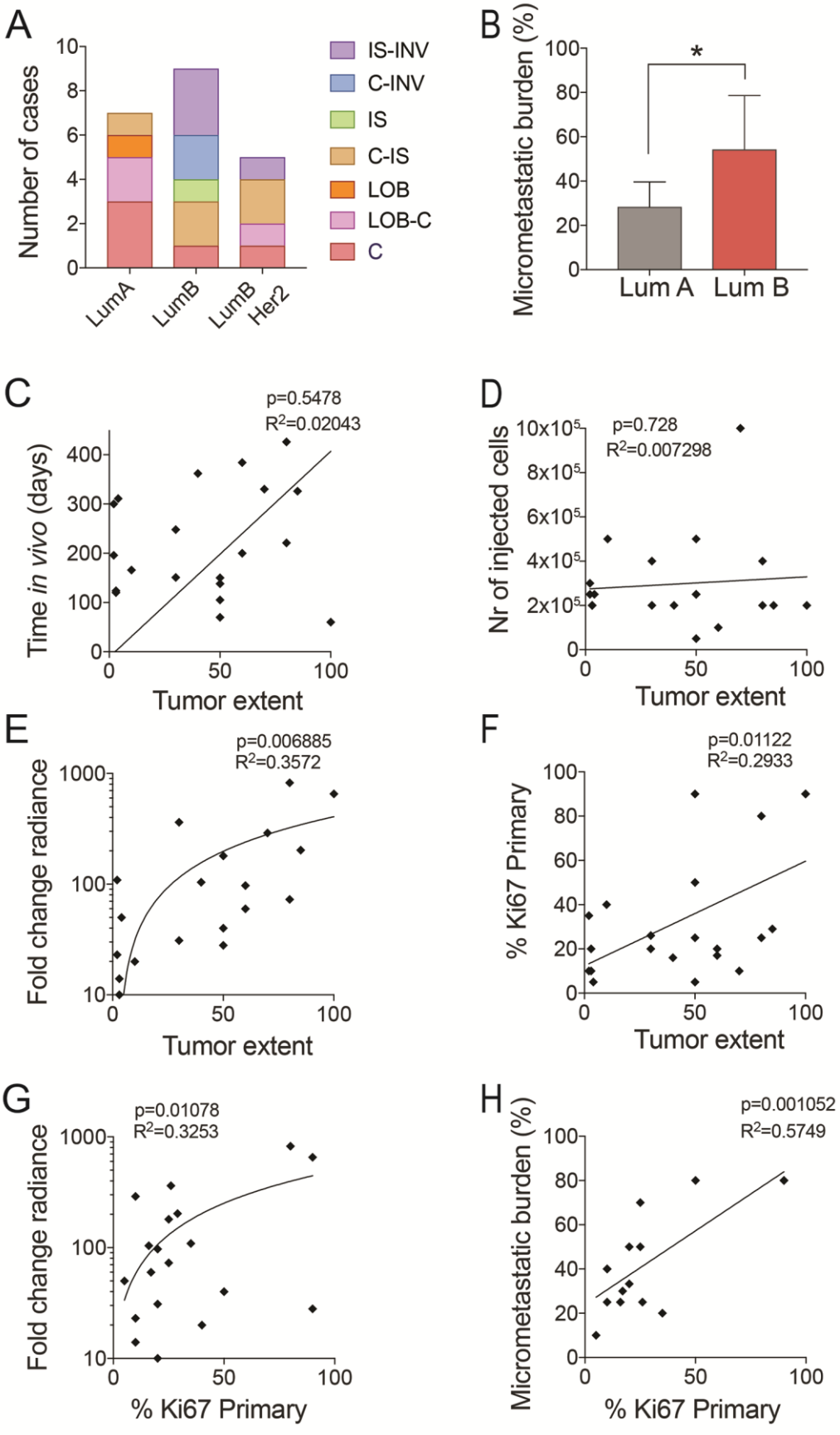

SUPPLEMENTARY MATERIAL ONLINE

Supplementary materials and methods **NO**

Supplementary figure legends **NO these are embedded in the figures**

Figure S1. Different tumor extents in PDXs.

Figure S2. Marker expression.

Figure S3. Human cells colonize mouse milk duct.

Table S1. Characterization of primary tumors (PTs) and PDXs.

Acknowledgements

We thank the Pathology Institute of the University Hospital of Lausanne (CHUV, Centre Hospitalier Vaudois) for its contribution to collecting and characterizing the primary tumors.

Author contributions

AT, AS, KZ, and RLS selected patients for participation in the study, obtained informed consent, and participated in planification of tumor collection with LB. VS, PA, AA, VD, GS performed experiments and analyzed data. MF took tumor samples, MF and GS analysed PDXs sections, MF and CB wrote the manuscript. All authors were involved in writing the paper and had final approval of the submitted and published versions. The work was supported by the Swiss Cancer Ligue KFS-3701-08-2015 and by Biltema and ISREC Foundation.

More information about the model can be found at https://brisken-lab.epfl.ch/PreclinicalModelCourse.

References

1 Ginsburg O, Bray F, Coleman MP, *et al.* The global burden of women's cancers: a grand challenge in global health. *Lancet* 2017; **389**: 847-860.

2 Howlader N, Altekruse SF, Li CI, *et al.* US incidence of breast cancer subtypes defined by joint hormone receptor and HER2 status. *J Natl Cancer Inst* 2014; **106:** 1-8.

3 Perou CM, Sørlie T, Eisen MB, *et al.* Molecular portraits of human breast tumours. *Nature* 2000; **406**: 747-752.

4 Nielsen TO, Parker JS, Leung S, *et al.* A comparison of PAM50 intrinsic subtyping with immunohistochemistry and clinical prognostic factors in tamoxifen-treated estrogen receptor-positive breast cancer. *Clin Cancer Res* 2010; **16**: 5222-5232.

5 Metzger-Filho O, Sun Z, Viale G, *et al.* Patterns of recurrence and outcome according to breast cancer subtypes in lymph node-negative disease: results from international breast cancer study group trials VIII and IX. *J Clin Oncol* 2013; **31**: 3083-3090.

6 Colleoni M, Sun Z, Price KN, *et al.* Annual hazard rates of recurrence for breast cancer during 24 years of follow-up: Results From the International Breast Cancer Study Group Trials I to V. *J Clin Oncol* 2016; **34**: 927-935.

7 Ma CX, Bose R, Ellis MJ. Prognostic and predictive biomarkers of endocrine responsiveness for estrogen receptor positive breast cancer. *Adv Exp Med Biol* 2016; **882**: 125-154.

8 Dobrolecki LE, Airhart SD, Alferez DG, *et al.* Patient-derived xenograft (PDX) models in basic and translational breast cancer research. *Cancer Metastasis Rev* 2016; **35**: 547-573.

9 Sflomos G, Dormoy V, Metsalu T, *et al.* A preclinical model for ERα-positive breast cancer points to the epithelial microenvironment as determinant of luminal phenotype and hormone response. *Cancer Cell* 2016; **29**: 407-422.

10 Richard E, Grellety T, Velasco V, *et al.* The mammary ducts create a favourable microenvironment for xenografting of luminal and molecular apocrine breast tumours. *J Pathol* 2016; **240**: 256-261

11 Lakhani S, Ellis I, Schnitt S, et al. WHO Classification of Tumours of the Breast. 4th ed. Lyon: IARC Press; 2012.

12 Oyama T, Maluf H, Koerner F. Atypical cystic lobules: an early stage in the formation of low-grade ductal carcinoma in situ. *Virchows Arch Int J Pathol* 1999; **435**: 413-421

13 Azzopardi JG. Benign and malignant proliferative epithelial lesions of the breast; a review. *Eur J Cancer Clin Oncol* 1983; **19**: 1717-1720.

14 Brogi E, Oyama T, Koerner FC. Atypical cystic lobules in patients with lobular neoplasia. *Int J Surg Pathol* 2001; **9**: 201-206.

15 Abdel-Fatah TMA, Powe DG, Hodi Z, *et al.* High frequency of coexistence of columnar cell lesions, lobular neoplasia, and low grade ductal carcinoma in situ with invasive tubular carcinoma and invasive lobular carcinoma. *Am J Surg Pathol* 2007; **31**: 417-426.

16 Curigliano G, Burstein HJ, Winer EP, *et al.* De-escalating and escalating treatments for early-stage breast cancer: the St. Gallen International Expert Consensus Conference on the Primary Therapy of Early Breast Cancer 2017. *Ann Oncol* 2018; (In Press).

17 Bombonati A, Sgroi DC. The molecular pathology of breast cancer progression. *J Pathol* 2011; **223**: 307-317.